Neural–Electronic Inhibition Simulated With a Neuron Model Implemented in SPICE

Robert B. Szlavik, Abuhanif K. Bhuiyan, Anthony Carver, and Frank Jenkins

***Abstract*—There have been numerous studies presented in the literature related to the simulation of the interaction between biological neurons and electronic devices. A complicating factor associated with these simulations is the algebraic complexity involved in implementation. This complication has impeded simulation of more involved neural–electronic circuitry and consequently has limited potential advancements in the integration of biological neurons with synthetic electronics. In this paper, we describe a modification to a previously proposed SPICE based Hodgkin–Huxley neuron model that demonstrates more physiologically relevant electrical behavior. We utilize this SPICE based neuron model in conjunction with an external circuit that allows for artificial selective inhibition of neural spiking. The neural firing control scheme proposed herein would allow for action potential frequency modulation of neural activity that, if developed further, could potentially be applied to suppress undesirable neural activity that manifests symptomatically as the tremors or seizures associated with specific pathologies of the nervous system.**

***Index Terms*—Inhibition, neural-electronics, neuron model, SPICE.**

I. Introduction

THERE have been several studies presented in the literature that demonstrate proof of principle neural–electronic circuitry [1]. Some of these studies include simulations of neural detection using synthetic electronic circuitry [2], [3]. Additional studies include simulations of neural excitation using external electronics [4], [5]. The simplicity of the overall circuit topology is a common feature of the simulations presented in the above literature. The approach adopted in some of these studies involves solution of the circuit equations using conventional numerical ordinary differential equation solvers or circuit simulation software [3], [5]–[7]. Algebraic manipulation involves rewriting these equations in a form whereby the first derivatives are isolated on one side. This manipulation of the circuit equations can be a tedious process for all but the simplest circuit topologies. As the overall complexity of the network topology becomes more involved and as the number of nodes in the system increases, the conventional numerical solver approach rapidly becomes intractable necessitating an alternate implementation strategy. Simulation packages such as NEURON and GENESIS do not provide the capability of simulating biological neurons combined in circuits with synthetic electronic devices which precludes their use in the simulation of hybrid neural–electronic circuits. The GENESIS platform does provide some device objects for simulating voltage clamp circuits or spike generators but, as in the case of the NEURON simulator, it is not a general purpose circuit simulation tool [8], [9].

There have been various SPICE neuron models presented in the literature [10], [11]. These models are based on the Hodgkin–Huxley active membrane model [12]–[16]. In this study, we present a modified version of one of these SPICE based neuron models that demonstrates more physiologically relevant electrical behavior of the simulated neuron [10]. The model proposed herein exhibits realistic transmembrane resting potentials yielding a more representative simulation of the direct current characteristics of the active membrane [17]. The strategy utilized to achieve more realistic resting membrane potentials involves the dispensation of physiologically unrealistic polynomial approximations of the rate constants in the ion gating equations of the Hodgkin–Huxley model. The use of these polynomial approximations was necessary when computational cost precluded direct implementation in SPICE of the nonlinear equations associated with the rate constants. With the advent of more powerful computing devices, computational cost is no longer a decisive issue with respect to direct implementation of the nonlinear functions associated with the Hodgkin–Huxley model [12]–[16].

In this study, the Hodgkin–Huxley based SPICE model is utilized in conjunction with an external network to simulate a neuron where a feedback topology is implemented to selectively remove charge from the neuron. This neuron is subjected to an independent and constant pulse frequency charge injection stimulus that is sufficient to elicit an action potential. This stimulus is analogous to constant frequency excitatory inputs from presynaptic neurons or artificially injected constant amplitude and frequency stimulus current pulses. Charge is removed from the target neuron selectively under external independent control which results in an independently selective stifling of the action potential. The circuit presented demonstrates artificial neural–electronic inhibition implemented in the form of a neural–electronic circuit.

II. Method

A. Modified SPICE Neuron Model

A modified version of a SPICE-based neuron model was developed, implemented, and utilized in this study [10]. The basic interface diagram for the spice model is illustrated in Fig. 1. Sodium and potassium Nernst potentials, based on ionic concentrations inside and outside the cell, are represented in the

Manuscript received December 13, 2004; revised September 19, 2005; accepted November 11, 2005.

R. B. Szlavik, A. Carver, and F. Jenkins are with the College of Engineering Science, Louisiana Tech University, Ruston, LA 71272 USA.

A. K. Bhuiyan is with Aster Telesolutions, Milpitas, CA 95035 USA.

Digital Object Identifier 10.1109/TNSRE.2006.870499

1534-4320/$20.00 © 2006 IEEE

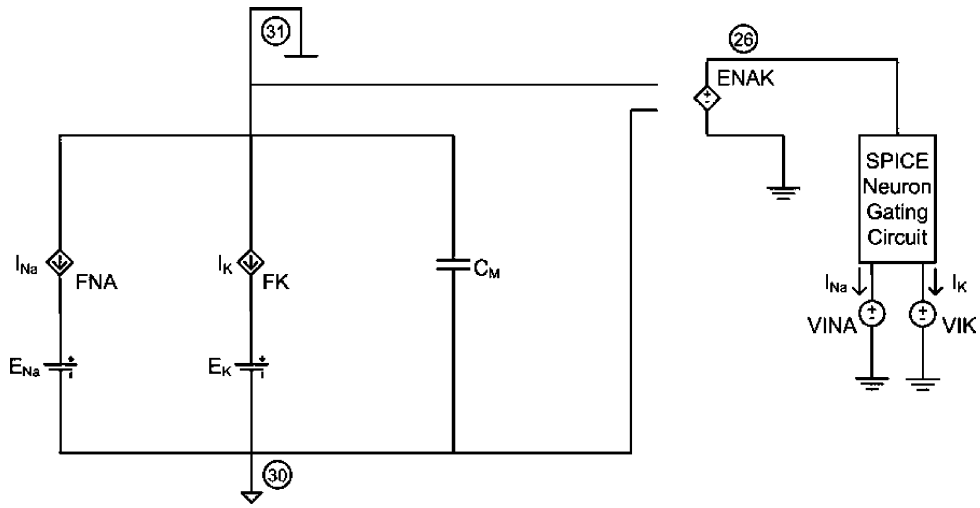

Fig. 1. SPICE neuron interface circuit. Above circuit diagram shows the connections between the neuron sub-circuit model and the rest of the SPICE simulation. Nodes 31 and 30 represent the intracellular and extracellular potentials, respectively. A voltage controlled voltage source, at node 26, provides the transmembrane potential information to the neuron gating circuit shown in Fig. 2 and the neuron gating circuit returns the sodium and potassium membrane current I_{Na} and I_K, respectively. Membrane capacitance is represented by C_M and the Nernst potentials for sodium and potassium are represented by E_{Na} and E_K, respectively.

sub-circuit model by the sources E_{Na} and E_K, respectively. The membrane capacitance is represented by C_M. The *ENAK* voltage controlled voltage source has a unitary gain and senses the potential across the neural membrane in the neuron interface circuit and generates an equivalent potential across the neuron gating circuit shown in Fig. 2. Sodium and potassium ionic current magnitudes are generated by the neuron gating circuit. These currents are detected by zero potential generators *VINA* and *VIK* for sodium and potassium, respectively, in the neuron gating circuit. The current values are regenerated in the neuron interface circuit of Fig. 1 through the current controlled current sources *FNA* and *FK*. Ionic current from the current controlled current source *FNA* and *FK* result in the generation of the associated transmembrane potential across the membrane nodes 31 and 30.

The neuron gating circuit reproduces the activity of the m, h, and n gates associated with the Hodgkin–Huxley active membrane model. The rate constants α_n and β_n, associated with the activity of the n gate, are established by the voltage controlled voltage sources *EAN* and *EBN*, respectively. These controlled voltage sources generate an output across nodes 9 and 10, respectively, based on the transmembrane potential control voltage that is generated at node 26. The rate constant equations are shown in (1) and (2) where V_m in these equations is the transmembrane potential in millivolts. Both of these equations contain terms associated with the transmembrane potential V_m which is implemented in the voltage controlled voltage source through the control potential at node 26

$$\alpha_n = \frac{-0.01 \cdot (V_m + 50)}{e^{[-0.1 \cdot (V_m + 50)]} - 1} \tag{1}$$

$$\beta_n = 0.125 \cdot e^{[-0.0125 \cdot (V_m + 60)]}. \tag{2}$$

The rate constants associated with the m and h gates are shown in (3)–(6)

$$\alpha_m = \frac{-0.1 \cdot (V_m + 35)}{e^{[-0.1 \cdot (V_m + 35)]} - 1} \tag{3}$$

$$\beta_m = 4 \cdot e^{((-V_m + 60)/18)} \tag{4}$$

$$\alpha_h = 0.07 \cdot e^{[-0.05 (V_m + 60)]} \tag{5}$$

$$\beta_h = \frac{1}{1 + e^{[-0.1 \cdot (V_m + 30)]}}. \tag{6}$$

The voltage controlled current sources *GAN* and *GBN* along with the capacitor that is connected to node 4 implement the rate equation associated with the n gate as shown in (7). The capacitor provides the differential operation associated with the potential at node 4 which is the n gating variable. The other terms in the equation are formed using the polynomial feature available in SPICE

$$\frac{dn}{dt} = \varphi \cdot \alpha_n (1 - n) - \varphi \cdot \beta_n n. \tag{7}$$

Temperature dependence of the Hodgkin–Huxley model is included using the scaling constant φ. The rate equations associated with the other two gating variables m and h are shown in (8) and (9), respectively

$$\frac{dm}{dt} = \varphi \cdot \alpha_m (1 - m) - \varphi \cdot \beta_m m \tag{8}$$

$$\frac{dh}{dt} = \varphi \cdot \alpha_h (1 - h) - \varphi \cdot \beta_h h. \tag{9}$$

The gating variable n at node 4 is used as the control voltage for the voltage controlled voltage source *EN4*. This controlled source is used to generate a potential that is equivalent to the fourth power of the n gating variable. The voltage controlled current source *GK* takes, as control inputs, n^4, as well as the difference between the transmembrane potential V_m and the Nernst equilibrium potential for potassium E_K. A voltage controlled voltage source *EMK* is used to generate a potential at node 17 equivalent to $(V_m - E_K)$. The voltage controlled current source *GK* is used to generate a current equivalent to the total potassium ionic current using the SPICE polynomial feature. A current is generated by this controlled source that is equivalent to $\overline{G}_K \cdot n^4 (V_m - E_K)$, where $\overline{G}_K$, computed for the cell surface area as per Table I, is the maximum potassium conductance in

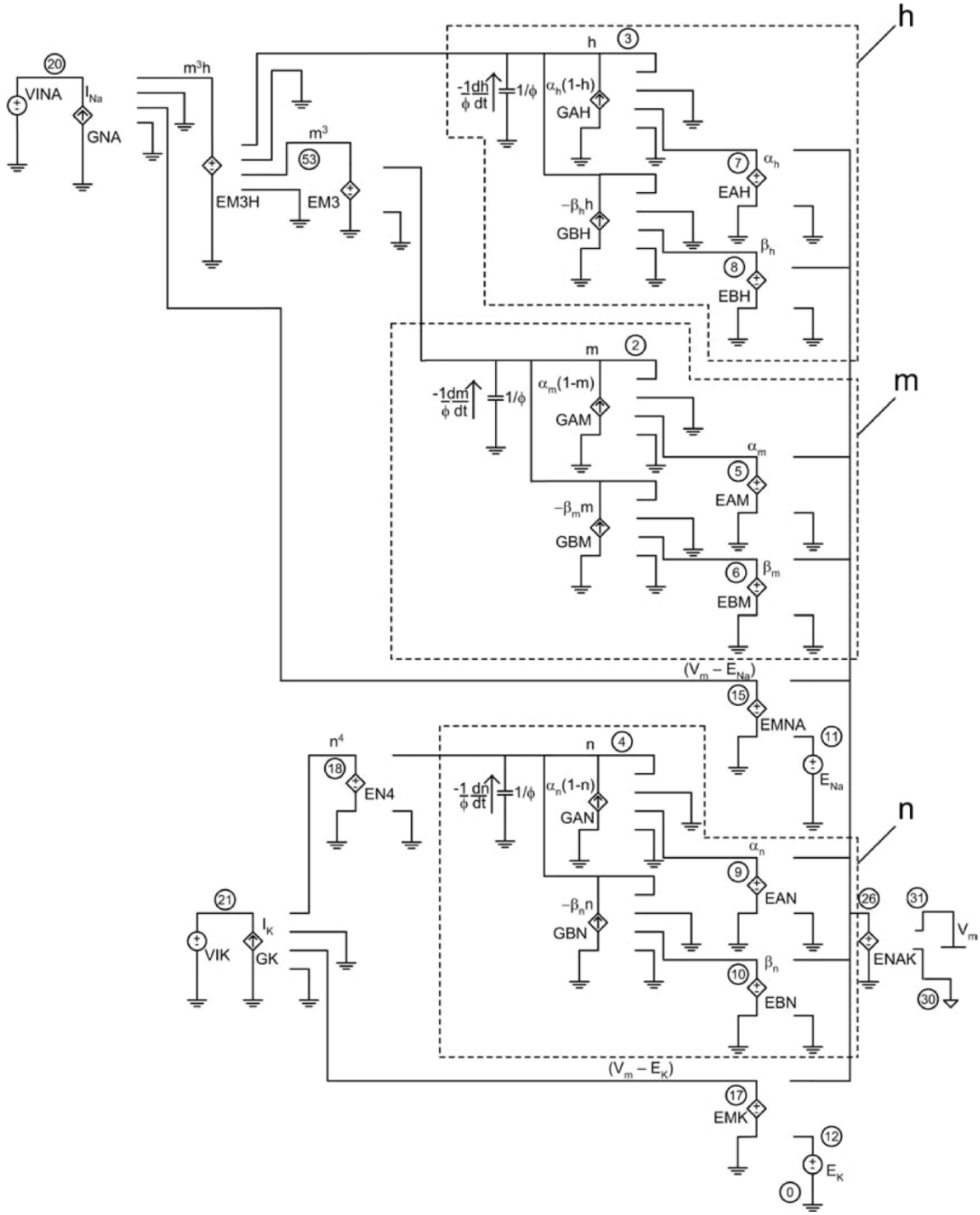

Fig. 2. SPICE neuron gating circuit. The m, h, and n gating variables are evaluated dynamically by the regions that are segmented in the circuit diagram by broken lines. Ionic current magnitudes for sodium and potassium are generated by the current controlled current sources *GNA* and *GK*, respectively. These currents are detected by the zero volt independent sources *VINA* and *VIK*. Input to the circuit is the transmembrane potential reproduced by the voltage controlled voltage source *ENAK*. Detailed explanation is provided in the text. In each case, for a controlled source, the value of the voltage or current associated with the source is shown in close proximity to the controlled generator.

Siemens. A similar approach is used to generate the sodium current.

B. Neural Electronic Inhibition Circuit

The strategy used to develop an external neural–electronic control loop that demonstrates artificial inhibition of neural activity relies on injected charge manipulation associated with a target cell. An overview of the control strategy is illustrated in Fig. 3.

It is assumed that the target cell is an electrically small cell. Consequently, the transmembrane potential is the same everywhere inside the cell which is further assumed to be cylindrical

TABLE I
LIST OF THE PHYSICAL AND GEOMETRIC PARAMETERS THAT WERE USED IN THE EQUIVALENT CIRCUIT MODELS AND THE SIMULATION STUDY

a	Cylindrical cell radius	**10 μm**
L	Cylindrical cell length	**80 μm**
$c_{Na}{}^{o}$	Extracellular sodium ion concentration	**0.491 (mol/L)**
$c_{Na}{}^{i}$	Intracellular sodium ion concentration	**0.05 (mol/L)**
$c_{K}{}^{o}$	Extracellular potassium ion concentration	**0.02011 (mol/L)**
$c_{K}{}^{i}$	Intracellular potassium ion concentration	**0.400 (mol/L)**
$G_{Na}{}^{M}$	Maximum sodium conductance per unit area	**0.120 (S/cm^2)**
$G_{K}{}^{M}$	Maximum potassium conductance per unit area	**0.036 (S/cm^2)**
T	Temperature	**6.3 (°C)**
c_M	Membrane capacitance per unit area	**1 μF/cm^2**

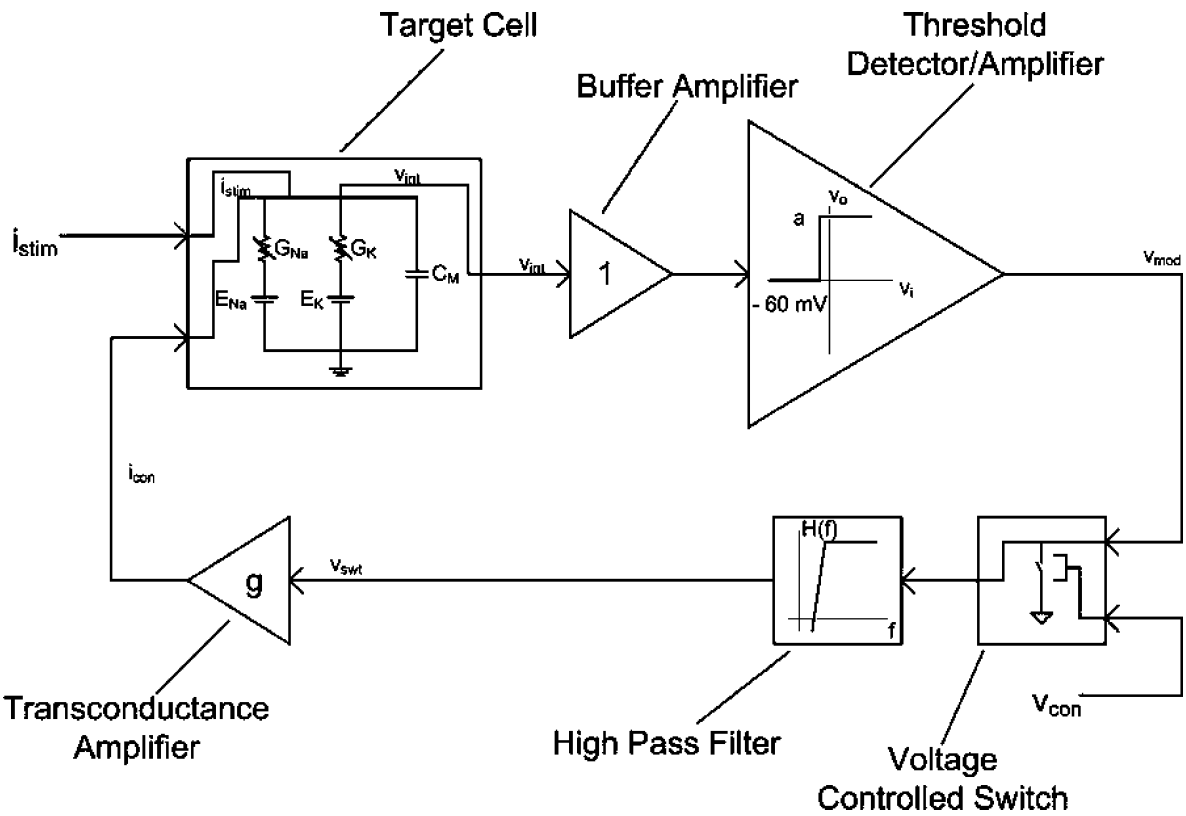

Fig. 3. Block diagram of neural–electronic inhibition control loop. A cylindrical electrically small target cell is represented by the Hodgkin–Huxley active membrane model described above where the cell is subjected to a constant repetitive stimulus current pulse $i_{\rm stim}$ of 10 mA/cm^2 with a duration of 2 μs and an inter-pulse period of 20 ms which is sufficient to generate an action potential under normal conditions. A control voltage $v_{\rm con}$ between 0 and 5 V is used to selectively inhibit the generation of an action potential by the target cell where a potential of 5 V turns on inhibition. Details of the circuit operation are described in the text.

with a diameter of 20 μm and a length of 80 μm, as indicated in Table I. A current pulse train external stimulus $i_{\rm stim}$ with an amplitude of 10 mA/cm^2, a pulsewidth of 2 μs, and an inter-pulse period of 20 ms is used to repetitively excite the target neuron. This constant external stimulus is sufficient to excite an action potential in the target cell. A control input $v_{\rm con}$ is used to turn on the neural–electronic artificial inhibitory effect. The control input consists of a potential between 0 and 5 V where a high potential of 5 V inhibits firing of the target cell.

A circuit simulation was implemented based on the block diagram shown in Fig. 3. Fig. 4 shows the schematic diagram of the circuit that was implemented in SPICE to verify the functionality of the proposed neural–electronic artificial inhibition system. An independent current source was used to generate the constant, fixed frequency stimulus. The unity gain buffer amplifier was implemented using the voltage controlled voltage source primitive circuit element configured with unity gain. An LM324 operational amplifier model (National Semiconductor), in conjunction with an independent voltage source set to -60 mV, was used to implement the threshold detector/amplifier stage.

III. RESULTS

The circuit shown in Fig. 3 was implemented in a SPICE netlist file and simulated using the student version of OrCAD PSPICE 9.1. Results from a transient response simulation were saved to an output text file and this file was used to generate the graphs. Figs. 5 and 6 show the results from a 200-ms transient response simulation. The neuron is repetitively excited by

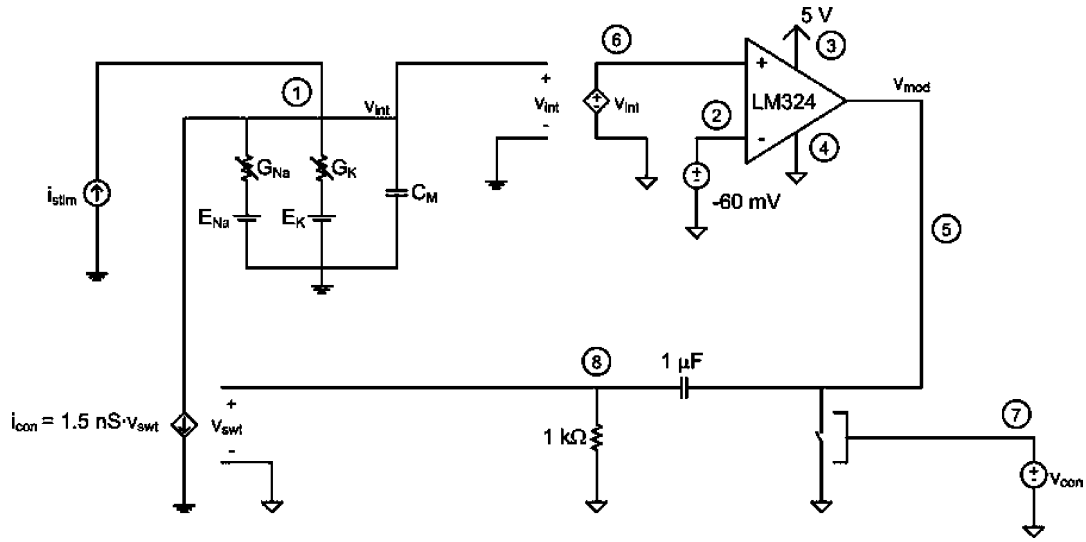

Fig. 4. SPICE circuit implementation of the neural–electronic inhibition control loop. Circuit shows an implementation of the conceptual block diagram shown in Fig. 3. A Hodgkin–Huxley active membrane equivalent circuit model, discussed earlier, is included in this simulation as a subcircuit, as is the LM324 operational amplifier model (National Semiconductor).

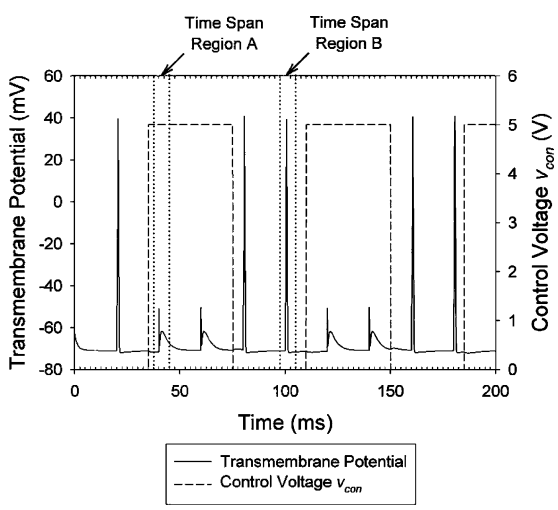

Fig. 5. Plot of the transmembrane potential and the control voltage $v_{\rm con}$. Transmembrane action potentials are extinguished during the activation of the inhibition control potential $v_{\rm con}$.

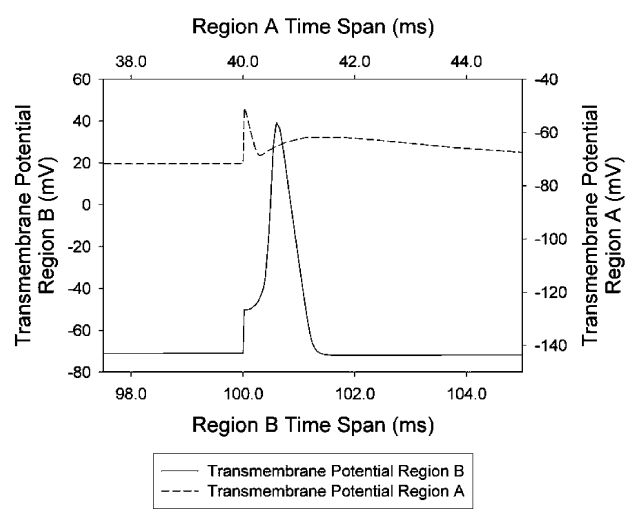

Fig. 6. Plot of the transmembrane potential for two different time spans. Graph shows a close up view of the normal uninhibited spiking activity observed when the artificial inhibition is off in Region B and when artificial inhibition is engaged in Region A. Region A vertical axis is shifted relative to region B for a clearer representation of the capacitive spiking.

the external fixed frequency current source $i_{\rm stim}$. Selective inhibition of neuron firing is activated by the control voltage $v_{\rm con}$ at 35 ms. The selective inhibition remains on for 40 ms and is turned off at 75 ms. During the period of time that selective inhibition is enabled, the action potential train generated by the target cell disappears.

The smaller spikes that are observed during the controlled inhibition period are associated with the transmembrane capacitance and the potential that develops across the transmembrane capacitance as a result of the injected charge from the repetitive excitation current stimulus $i_{\rm stim}$. Once the selective artificial inhibition is turned off at 75 ms, normal spiking activity of the target cell resumes in response to the fixed frequency external current stimulus $i_{\rm stim}$.

The amplitude of transmembrane capacitive spikes can be calculated from the charge potential relationship of a capacitor. A value for the charge per unit area injected from the stimulus current pulse can be determined by integrating the 2-μs stimulus current pulse with respect to time which yields a value of the injected charge of 20 $\rm nC/cm^2$. Given a membrane capacitance of 1 $\mu\rm F/cm^2$, the resultant potential change across the transmembrane capacitance should be approximately 20 mV which is consistent with the potential change associated with the smaller spikes observed at the onset of the stimulus current pulse in the simulation.

IV. Discussion

We have presented an improved electrical equivalent circuit representation of the Hodgkin–Huxley active membrane model. This circuit representation is based on the equivalent circuit developed earlier [10] and is suitable for implementation in

SPICE. The circuit representation herein does not rely on polynomial approximations of the gating variable rate constants but incorporates the nonlinear exponential functions that describe the gating variable rate constants' dependence on the transmembrane potential. A principal improvement over previous models is that our model demonstrates potential variations and levels that are consistent with the expected physiological behavior of electrically active cell membranes. To improve the versatility of the model, we implemented it in the form of a SPICE sub circuit. A sub-circuit representation improves the portability and ease of integration into larger SPICE network simulation studies.

A design of an external artificial inhibitory neural–electronic system was proposed that included an electrical representation of a neuron that was implemented with the improved model described herein. The overriding principle behind the proposed control loop is the selective removal of charge from a target cell that is subjected to a repetitive and constant current stimulus capable of exciting an action potential in the cell. It was demonstrated that, in the simulation study, artificial external inhibition of the action potential spiking activity of the target neuron can be controlled by an externally applied control voltage.

While the charge removal system that has been proposed would be most applicable in the context of a laboratory experiment to control spiking activity of cells *in vitro*, the concept could potentially be extended to clinical applications. This study demonstrated that it is possible to selectively control the action potential activity artificially which suggests that it should be possible to artificially modulate the action potential pulse frequency in a neuron. If neural pulse frequency modulation could be achieved in an *in vivo* environment, then such a system could be applied to the alleviation of aberrant spiking activity associated with specific neurological pathologies such as focal epilepsy arising from congenitally deranged circuitry localized on the cerebral cortex. A major impediment to this goal would be the translation of this concept from an experimental charge removal based quenching of the action potential to one where the action potential is extinguished by an electrode or other device placed in close proximity to the outside of the cell. A capacitance coupled neural–electronic transistor, such as the devices described by Fromherz and Stett [4], could potentially provide an alternative to invasive intracellular charge removal. Simulation studies necessary to test the concept of action potential quenching using a device external to the cell are currently underway.

REFERENCES

[1] S. Vassanelli and P. Fromherz, "Neurons from rat brain coupled to transistors," *Appl. Phys. A Solids Surf.*, vol. 65, pp. 85–88, 1997.

[2] R. Weis and P. Fromherz, "Frequency dependent signal transfer in neuron transistors," *Phys. Rev. E, Statist. Phys. Plasmas Fluids Relat. Interdiscip. Top.*, vol. 55, no. 1, pp. 877–889, Jan. 1997.

[3] R. B. Szlavik, "Strategies for improving neural signal detection using a neural–electronic interface," *IEEE Trans. Neural Syst. Rehabil. Eng.*, vol. 11, no. 1, pp. 1–8, Mar. 2003.

[4] P. Fromherz and A. Stett, "Silicon-neuron junction: Capacitive stimulation of an individual neuron on a silicon chip," *Phys. Rev. Lett.*, vol. 75, no. 8, pp. 1670–1673, 1995.

[5] R. B. Szlavik and F. Jenkins, "Varying the time delay of an action potential elicited with a neural–electronic stimulator," in *Proc. IEEE EMBS Conf.*, vol. 2, San Francisco, CA, 2004, pp. 4353–4355.

[6] R. B. Szlavik, "The impact of variations in membrane capacitance on the detected neural–electronic signal," in *Proc. IEEE EMBS Conf.*, vol. 3, Houston, TX, 2002, pp. 2095–2096.

[7] ——, "Semiconductor laser diode gain switching techniques and laser diode equivalent circuit modeling in SPICE," M.Eng. thesis, McMaster Univ., Hamilton, ON, Canada, 1993.

[8] M. Hines and N. Carnevale, "Computer simulation methods for neurons," in *The Handbook of Brain Theory and Neural Networks*, 2nd ed, M. Arbib, Ed. Cambridge, MA: MIT Press, 2002.

[9] M. Hines, "NEURON—A program for simulation of nerve equations," in *Neural Systems: Analysis and Modeling*, F. Eeckman, Ed. Norwell, MA: Kluwer, 1993.

[10] B. Bunow, I. Segev, and J. W. Fleshman, "Modeling the electrical behavior of anatomically complex neurons using a network analysis program: Excitable membrane," *Biol. Cybern.*, vol. 53, pp. 41–56, 1985.

[11] M. Bove, G. Massobrio, S. Martinoia, and M. Grattarola, "Realistic simulations of neurons by means of an ad hoc modified version of SPICE," *Biol. Cybern.*, vol. 71, pp. 137–145, 1994.

[12] A. L. Hodgkin and A. F. Huxley, "A quantitative description of membrane current and its application to conduction and excitation in nerve," *J. Physiol.*, vol. 117, pp. 500–544, 1952.

[13] ——, "The components of membrane conductance in the giant axon of loligo," *J. Physiol.*, vol. 116, pp. 473–496, 1952.

[14] ——, "The dual effect of membrane potential on sodium conductance in the giant axon of loligo," *J. Physiol.*, vol. 116, pp. 497–506, 1952.

[15] A. L. Hodgkin, A. F. Huxley, and B. Katz, "Measurement of current-voltage relations in the membrane of the giant axon of loligo," *J. Physiol.*, vol. 116, pp. 424–448, 1952.

[16] A. L. Hodgkin and A. F. Huxley, "Currents carried by sodium and potassium ions through the membrane of the giant axon of loligo," *J. Physiol.*, vol. 116, pp. 449–472, 1952.

[17] E. Kandel, J. Schwartz, and T. Jessell, *Principles of Neural Science*, 4 ed. New York: McGraw Hill, 2000.

Robert B. Szlavik received the B.Eng. (*summa cum laude*), M.Eng., and Ph.D. degrees in electrical and computer engineering from McMaster University, Hamilton, ON, Canada, in 1991, 1994, and 1999, respectively.

He is currently Program Chair of Electrical Engineering at Louisiana Tech University, Ruston. He is affiliated with the Center for Biomedical Engineering and Rehabilitation Science (CyBERS), also at Louisiana Tech University. He has served as a Scientific Consultant to the U.S. Food and Drug Administration, Center for Devices and Radiological Health. His research interests are in the areas of neural–electronics and the mathematical modeling of the electrical behavior of neurological systems.

Abuhanif K. Bhuiyan received the B.Eng. degree in avionics engineering on a scholarship from the College of Aeronautical Engineering, Risalpur, Pakistan, in 1996, and the M.S. degree in electrical engineering from Louisiana Tech University, Ruston, in 2004.

He retired from the Bangladesh Air Force with the rank of Flight Lieutenant in 2001. Presently, he is an Engineer with Aster Telesolutions, Milpitas, CA.

Anthony S. Carver received the B.S. degree in computer science from Angelo State University, San Angelo, TX, in 1998 and the M.S. degree in microsystems engineering from Louisiana Tech University, Ruston, in 2005, where he is currently working toward the Ph.D. degree under Dr. R. B. Szlavik.

He is also an active duty Captain in the U.S. Air Force working as a Developmental Engineer. His research interests are in the areas of neural–electronics and the mathematical modeling of the electrical behavior of neurological systems.

Frank Jenkins received the B.Eng. degree in chemical engineering from Washington State University, Pullman, in 1994. He is currently working toward the Ph.D. degree in engineering at Louisiana Tech University, Ruston.

His research interests are in the areas of neural–electronics and the mathematical modeling of the electrical behavior of neurological systems, and chemical reaction networks.